Catalysis Today 155 (2010) 214–222

Contents lists available at ScienceDirect

Catalysis Today

journal homepage: www.elsevier.com/locate/cattod

Specific insight of active sites in $Cs_2Te_xV_yPMo_{12}O_{40}$ catalysts efficient for selective oxidation of isobutane by operando resonance Raman spectroscopy

Stéphane Loridant *, Quyen Huynh, Jean-Marc M. Millet

Institut de Recherches sur la Catalyse et l'Environnement de Lyon, IRCELYON, UMR5256 CNRS-Université Claude Bernard Lyon 1, 2 av. Einstein, F-69626 Villeurbanne Cedex, France

ARTICLE INFO

Article history:
Available online 18 November 2009

Keywords:
Keggin-type phosphomolybdate
Tellurium
Vanadium
Reduced heteropolyanion
Resonance Raman spectroscopy
Operando Raman spectroscopy
Active sites

ABSTRACT

Keggin-type phosphomolybdates with cesium, tellurium and vanadium as counter-cations, recently shown to be efficient for selective oxidation of isobutane, were characterized by diffuse reflectance and Raman spectroscopy. In the present study, it was shown that the Raman bands appearing in addition to those of $[PMo_{12}O_{40}]^{3-}$ in these catalysts after reaction were observed with much better sensitivity using exciting lines at 647.1 and 785 nm. This phenomenon, linked to the existence of d–d transitions and intervalence charge transfers at 680 and 860 nm, respectively, arises mainly from reduction of the probed depth and to a lesser extent, from enhancement effect using resonance Raman spectroscopy. The better sensitivity of this technique was used to follow specifically the additional bands before, during and after reaction. They were attributed to highly reduced phosphomolybdates stabilized under reaction mixture and possibly capped by Te^{4+} and $(V{=}O)^{2+}$. The reduced species would be present in a layer lying over unreduced Keggin salt and specifically probed using resonance Raman spectroscopy. Substitution by tellurium cations was shown to favour reduction of Keggin heteropolyanions under reaction mixture. Operando resonance Raman experiments evidenced that, for the samples without vanadium, reduced phosphomolybdates were formed above 120 °C during the raise up to the reaction temperature whereas for the samples with vanadium, small amount of these species was already observed before reaction because of oxidation of V^{3+} to V^{4+} cations during drying. This amount also increased during the thermal activation under reaction feed. The relative intensity of the additional bands was maximal when the catalysts were active and selective under reaction mixture. After reaction, this parameter was related to the selectivity to methacrolein and methacrylic acid suggesting that reduced phosphomolybdates are more selective active sites.

1. Introduction

The operando methodology is powerful to establish relationships between catalytic activity and catalyst structure by coupling characterization experiments and catalytic measurements in a same cell. It is a tool to design and prepare better catalysts [1–3]. However, in heterogeneous catalysis, it is sometimes difficult to identify active sites because they are located at the surface of catalysts and can be present in very limited number. Therefore, well-chosen techniques are required to determine the structure of these sites. Resonance Raman spectroscopy allows observation of diluted chromophores enhancing bands of molecules or crystals owning electronic transition in the UV–near IR range when the wavelength of the laser exciting line coincides with that of the transition. Additionally, resonance Raman spectroscopy probes much less layers of matter than other bulk techniques since the resonance process is often associated with strong (re)-absorption [4,5]. Therefore, it can be key technique to characterize catalytic active sites as previously illustrated in the literature [6–10].

Recently, new catalysts based on phosphomolybdic acid substituted by cesium, tellurium and vanadium cations were shown to be efficient and stable for selective oxidation of isobutane to methacrylic acid [11]. This direct reaction is particularly attractive to replace the current "acetone–cyanohydrin" process that generates numerous toxic wastes [12]. Incorporation of tellurium led to improved selectivity to methacrylic acid and incorporation of vanadium to improved catalytic activity [13].

The catalysts had been characterized by various bulk techniques before and after reaction revealing limited features. Indeed, XRD patterns only revealed a cubic structure typical of cesium heteropolysalt and IR spectra only contained vibration bands typical of $[PMo_{12}O_{40}]^{3-}$ Keggin anions. However, X-absorption spectroscopies were much more informative since the oxidation state of both tellurium and vanadium was determined to be IV

---

* Corresponding author. Tel.: +33 (0)4 72 44 53 34; fax: +33 (0)4 72 44 53 99.
E-mail address: stephane.loridant@ircelyon.univ-lyon1.fr (S. Loridant).

0920-5861/$ – see front matter © 2009 Elsevier B.V. All rights reserved.
doi:10.1016/j.cattod.2009.10.009

before and after reaction and the presence of [TeO_4] clusters capping Keggin anions has been proposed [13]. Raman spectra of the catalysts achieved before reaction with exciting line at 514.5 nm were typical of Keggin units with cesium as counter-cations [14]. However, small additional bands were evidenced after reaction for the best compounds [13]. These bands cannot be attributed to any allotropic form of MoO_3 nor to fragments of Keggin units as previously described [15].

In this paper, enhancement of additional bands by resonance effect has been evidenced using exciting lines at 647.1 and 785 nm. The use of resonance Raman spectroscopy allowed specific insight of the corresponding species thanks to much better sensitivity. From visible diffuse reflectance spectra, this better sensitivity was explained at first by strong re-absorption using red or near IR exciting line and to a lesser extent by resonance effect. It allowed a more precise comparison of additional bands with reference spectra for attribution, to investigate the influence of the counter-cations composition on their intensity and to establish relationships with catalytic properties. The formation of the corresponding species and their stability depending on the redox strength of the atmosphere were investigated achieving in situ and operando measurements.

2. Experimental

2.1. Preparation of the $Cs_2Te_xV_y$ catalysts and references

The catalysts were prepared substituting protons contained in phosphomolybdic acid by cesium, tellurium and vanadium cations [13] and were labelled according to their atomic counter-cations content ($Cs_2Te_xV_y$). During typical preparation, 8.16 g of $H_3PMo_{12}O_{40}\cdot xH_2O$ (Fluka, Ref. 79560) and various amounts of telluric acid were dissolved in 140 ml of deionised water. A second solution containing 1.3 g of Cs_2CO_3 in 0.4 ml of deionised water was added dropwise leading to the formation of a precipitate. The mixture was kept under stirring for 1 h at 80 °C before evaporation at reduced pressure using a rotavapor, was then dried at 125 °C and finally calcined under air flow at 360 °C for 6 h. The preparation of Cs_2Te_x samples was achieved at this step. To obtain the $Cs_2Te_xV_y$ samples, remaining protons were substituted by maintaining Cs_2Te_x salts in a solution of toluene containing vanadium acetylacetonate for 6 h under stirring at room temperature. Finally, the substituted solids were only dried under reduced pressure at 60 °C using a rotavapor. For testing measurements, the $Cs_2Te_xV_y$ samples were directly heated under reaction mixture.

$(MoO_2)_{0.5}(PMo_{14}O_{42})$ reference compound was obtained according to a procedure published by Marosi et al. [16,17] calcining the $(NH_4)_3PMo_{12}O_{40}\cdot xH_2O$ ammonium salt (Aldrich, Ref. 342165) under N_2 flow at 470 °C for 6 h. The XRD pattern of the prepared compounds was completely indexed with that of $(MoO_2)_{0.5}(PMo_{14}O_{42})$ (PDF-ICDD 056-0165). IR vibration bands of this sample were located at 1057, 1052, 1009, 994, 972, 961, 866, 786, 768, 715, 675, 579, 550, 534, 508, 466, 451, 440 and 423 cm^{-1}. Four electron reduced $(TBA)_7PMo_{12}O_{40}$ salt was also prepared by reduction of $H_3PMo_{12}O_{40}$ (Fluka, Ref. 79560) using $N_2H_4\cdot H_2O$ (Aldrich, Ref. 207942) in 50% dioxane–50% water solution followed by precipitation using TBABr salt (Fluka, Ref. 86857). The sample evidenced ^{31}P-NMR band at −13.3 ppm typical of β-IV reduced Keggin anion [18].

2.2. Characterization techniques

Raman experiments were achieved using UV–vis–NIR LabRam HR spectrometer (Horiba–Jobin Yvon) equipped with BXFM confocal microscope, interference and Notch filters and CCD detector cooled at −76 °C by Peltier effect. The diffused light was spatially dispersed with a 1800 grooves/mm or a 300 grooves/mm diffraction grating. The influence of the laser wavelength on the Raman spectra of catalysts has been investigated. For that purpose, the exciting lines at 457.9, 514.5 and 647.1 nm delivered by a 2018 RM Ar–Kr laser (Spectra physics) and the exciting line at 785 nm obtained from a diode laser were used. After evidencing resonance effect of additional bands both at 647.1 and 785 nm, the first one was preferred to the second one because black body emission is intense in near IR range even at moderate temperature and can limit in situ and operando experiments.

For all the exciting lines, an extreme care has been taken to choose a working laser power for which the heating effect was negligible. Therefore, the power at the samples was limited to only 100 μW for all the experiments. In that regard, it is important to mention that the enhancement of additional bands cannot be observed in ambient air using a too much high laser power because of the heating of samples.

An objective with magnification 100× was selected for ex situ measurements whereas a long working distance objective with magnification 50× was used for in situ and operando studies. During ex situ measurements, several areas were analysed under microscope for each composition. The comparison of spectra from one point to the other has shown good homogeneity of the catalysts before and after reaction.

In situ Raman spectra were recorded during thermal treatments of samples located in a crucible lying on the heating sole of a THMS600 cell linked a TMS94 programmer (Linkam). The set-up for operando experiments was previously described in detail [19]. It consists of a home-made furnace containing four heating plugs and fixed-bed quartz micro-reactor specially designed for such measurements. The last one contained a quartz window for light transmission, thermocouple hollow, inlet–outlet gas connections and a porous disc on which the investigated catalysts laid. The feedstock composition used for operando experiments was $27\%iC_4H_{10}/13.5O_2/10H_2O/49.5He$ and corresponded to an optimised mixture [13]. The temperature was varied from 20 °C up to 376 °C under a 20 ml min^{-1} gas flow at atmospheric pressure. iC_4H_{10} and O_2 conversions were determined using a VG ProLab mass spectrometer (Thermo Electron Corporation) located after the cell. Selectivities to methacrolein (MA) and methacrylic acid (MAA) products were obtained from gas chromatography analysis using a GC 2012 (Shimatzu) after ice-cooled trapping. They were calculated from the formula $S_i = n_i/\Delta n iC_4H_{10}$ where S_i is the selectivity to MA or MAA, n_i the number of moles produced during the time of trapping and $\Delta n iC_4H_{10}$ the number of moles of isobutane converted at the same time. CO and CO_2 products were detected with the mass spectrometer but not quantified. Traces of acetic acid were also formed during operando experiments.

Diffuse reflectance spectra were carried out on powders in the visible–near IR range using a Lambda 35 spectrometer (PerkinElmer) equipped with integrating sphere. A Spectralon® standard sample was used as reference. The spectra are reported using the Kubelka–Munk function given by $FR(\lambda) = (1 - R(\lambda))^2/2R(\lambda)$ where $R(\lambda)$ corresponds to the reflectance at the λ wavelength.

Chemical analysis of Mo, V, Te and P cations was obtained by atomic emission using an induced plasma technique and using an air–acetylene flame for Cs cations. X-ray diffraction patterns were achieved from 3° to 80° (2θ) with a step of 0.02° using a Siemens D5005 diffractometer and Cu Kα radiation. The ICDD database was used for indexation. Transmission FTIR spectra of samples dispersed in KBr were recorded with a Brüker Vector 22 spectrometer. Finally, ^{31}P-NMR spectra were acquired on a Bruker DSX 400 spectrometer.

3. Results

3.1. Electronic properties

Diffuse reflectance spectra of $Cs_2Te_{0.2}$ sample before and after reaction are plotted between 400 and 1000 nm in Fig. 1a and b, respectively. Before reaction, no bands were observed above 600 nm whereas two strong and broad absorption bands were evidenced at 680 and 860 nm after. These bands assigned to d–d and intervalence charge transfer (IVCT), respectively [20–23] revealed the presence of Mo^{5+} cations in the sample. The same features were observed for all the Cs_2Te_x samples after reaction. As illustrated in Fig. 1c with $Cs_2Te_{0.2}V_{0.1}$ sample, d–d and IVCT bands were already observed before reaction in vanadium containing samples contrary to samples without vanadium. This phenomenon can be explained by the preparation method of these catalysts. Indeed, it has been shown from XANES measurements that the average oxidation state of vanadium was IV after drying (i.e. before reaction) whereas it was III in the vanadium acetylacetonate precursor [13]. Hence, vanadium cations were oxidized during the drying involving probably reduction of some Mo^{6+} cations to Mo^{5+}. After reaction, higher FR values were measured above 600 nm indicating higher degree of reduction of the $Cs_2Te_{0.2}V_{0.1}$ sample (Fig. 1d).

Fig. 1e shows the diffuse reflectance spectrum of Cs_2H sample after reaction. By comparison with those of $Cs_2Te_{0.2}$ and $CsTe_{0.2}V_{0.1}$ samples (Fig. 1b and d, respectively), it appears that the d–d and IVCT bands of the two tellurium containing samples were much more intense than those of the Cs_2H sample indicating the presence of more reduced or a higher number of reduced molybdenum species. Hence, tellurium could favour reduction.

3.2. Influence of the laser wavelength on Raman spectra

It has been recently shown that, after reaction, small Raman bands appeared in addition to those of $[PMo_{12}O_{40}]^{3-}$ for all the tellurium containing samples using exciting line at 514.5 nm [13]. Having in mind that these features could arise from reduced species exhibiting the two absorption bands at 680 and 860 nm, the influence of the laser wavelength on the shape of Raman spectra was investigated looking for resonance effect.

The Raman spectra obtained with exciting lines at 457.9, 514.5, 647.1 and 785 nm on $Cs_2Te_{0.5}$ sample after reaction, are compared in Fig. 2. As expected, an impressive change of spectra was evidenced varying the exciting line from the violet to the near IR spectral range. Indeed, using the exciting line at 647.1 and 785 nm, the additional bands listed in bold in Table 1 were strongly enhanced compared to those of $[PMo_{12}O_{40}]^{3-}$ located at 988, 971, 959, 610, 385, 251 and 236 cm^{-1}. The additional bands were not observed for the sample before reaction. It can be related to the absence of electronic transition above 600 nm as mentioned in the previous part.

A possible explanation for the spectral evolution observed with the sample after reaction is a resonance effect. Indeed, the Raman intensity varies as the square of the derivative of polarisability that becomes high when the wavelength of the laser coincides with that of a dipole-allowed electronic transition. The Raman band of the vibrational mode giving the vibronic structure of the transition is

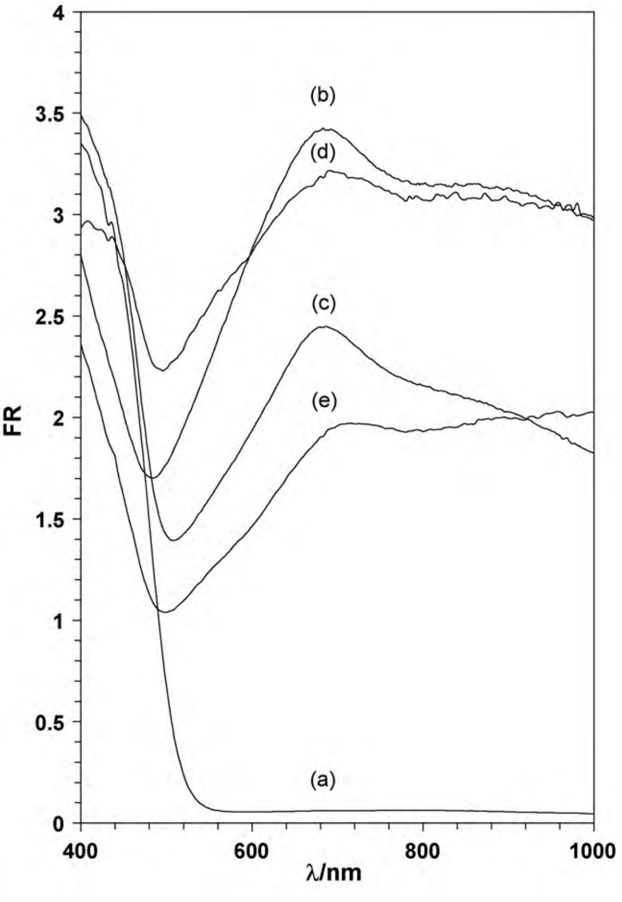

Fig. 1. Visible/near IR diffuse reflectance spectra of $Cs_2Te_{0.2}$ sample: (a) before and (b) after reaction, of $Cs_2Te_{0.2}V_{0.1}$ sample (c) before and (d) after reaction and of (e) Cs_2H sample after reaction.

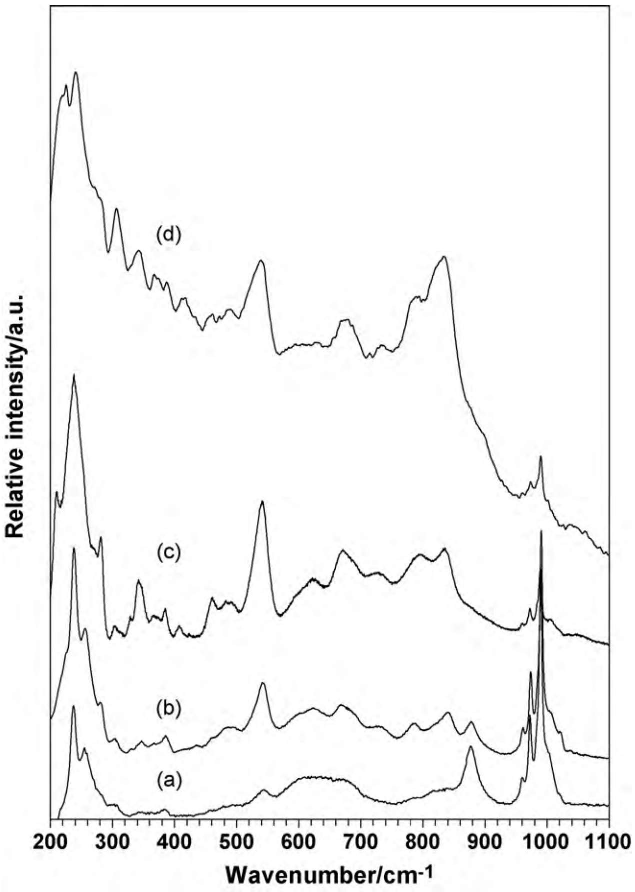

Fig. 2. Raman spectra of $Cs_2Te_{0.5}$ sample after reaction achieved with exciting line at: (a) 458 nm, (b) 514.5 nm, (c) 647.1 nm and (d) 785 nm.

Table 1
Wavenumbers and assignments of bands observed on Raman spectra of $\mathrm{Cs_2Te_{0.5}}$ sample after reaction achieved with exciting lines at 457.9, 514.5, 647.1 and 785 nm. Values in bold correspond to bands observed in addition to those of $[\mathrm{PMo_{12}O_{40}}]^{3-}$. vs: very strong, s: strong, m: medium, w: weak, and vw: very weak.

Wavenumbers ($\mathrm{cm^{-1}}$)				Assignments [24]
457.9 nm	514.5 nm	647.1 nm	785 nm	
1020	**1022**	**1020** (**vw**)		
1004	**1006**	**1010** (**w**)	**1001**	
990	990	988	990	$\nu_{\mathrm{s}}(\mathrm{Mo{-}O_{t}})$
972	974	971	974	$\nu_{\mathrm{as}}(\mathrm{Mo{-}O_{t}})$
962	962	959	963	$\nu_{\mathrm{as}}(\mathrm{Mo{-}O_{t}})$
			897	
879	878			$\nu_{\mathrm{as}}(\mathrm{Mo{-}O_{2c2}{-}Mo})$
	843	**839** (**s**)	**833**	
	787	**800** (**s**)	**788**	
	733	**734** (**s**)	**732**	
673	**673**	**675** (**s**)	**673**	
	625	**628** (**s**)		
610	610			$\nu_{\mathrm{s}}(\mathrm{Mo{-}O_{2c1}{-}Mo})$, $\delta(\mathrm{Mo{-}O_{2c1}{-}Mo})$
546	**545**	**543** (**vs**)	**540**	
		497 (**w**)		
	485	**487** (**w**)	**489**	
	461	**464** (**m**)	**462**	
		411 (**w**)	**415**	
382	389	385	388	$\delta(\mathrm{Mo{-}O_{2c2}{-}Mo})$
		370 (**w**)	**368**	
346	352			$\delta(\mathrm{Mo{-}O_{2c2}{-}Mo})$, $\delta(\mathrm{Mo{-}O_{2c1}{-}Mo})$
		345 (**s**)	**343**	
	330	**327** (**w**)		
300	**309**	**306** (**w**)	**307**	
	283	**282** (**m**)	**282**	
			272	
255	257	251		$\delta(\mathrm{O_{2c2}{-}Mo{-}O_{2c1}})$, $\delta(\mathrm{O_{2c2}{-}Mo{-}O_{2c2}})$
237	238	236	242	$\delta(\mathrm{Mo{-}O_{2c2}{-}Mo})$, $\nu_{\mathrm{s}}(\mathrm{Mo{-}O_{4c}})$

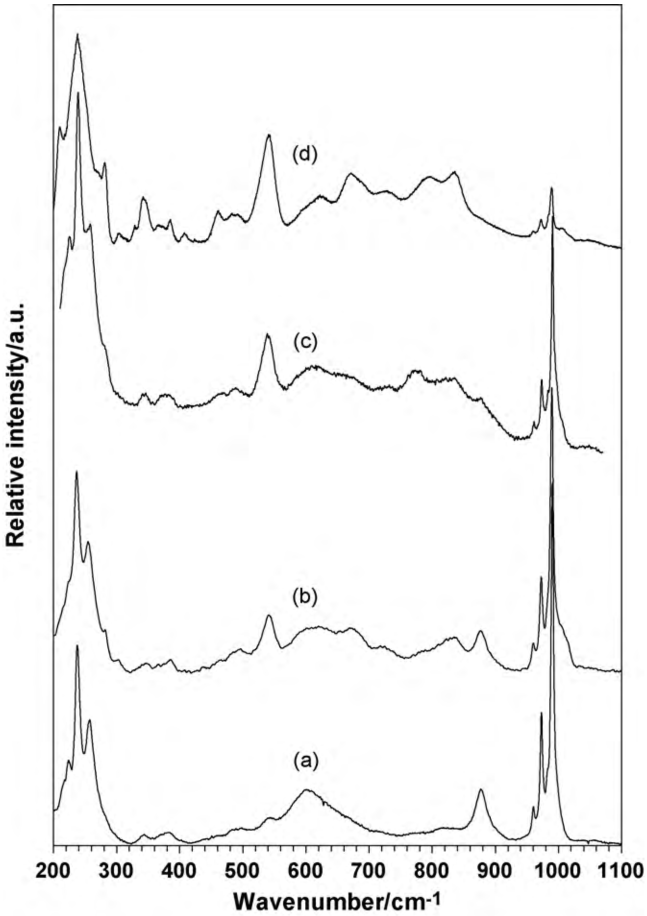

Fig. 3. Raman spectra of $\mathrm{Cs_2Te_{0.2}V_{0.1}}$ sample achieved with exciting line at 514.5 nm: (a) before and (b) after reaction and at 647.1 nm: (c) before and (d) after reaction.

often greatly enhanced [20]. In the present study, no additional band was specifically enhanced and hence, if resonance phenomena occurred, they cannot be associated with the same electronic transitions [20]. However, some variations in the relative intensities of additional bands can be noticed below 400 $\mathrm{cm^{-1}}$ depending on the laser wavelength. In particular, the band at 345 $\mathrm{cm^{-1}}$ was enhanced at 647.1 nm (Fig. 2c) whereas that at 307 $\mathrm{cm^{-1}}$ was much more intense at 785 nm (Fig. 2d). Finally, the δ(Mo–O–Mo) band around 240 $\mathrm{cm^{-1}}$ already present in $[\mathrm{PMo_{12}O_{40}}]^{3-}$ was much higher than the ν(Mo=O) bands above 960 $\mathrm{cm^{-1}}$ using exciting lines at 647.1 and 785 nm. This evolution could also be ascribed to weak resonance effect.

The second parameter that can explain the spectral evolution with the laser wavelength is the variation of the probing depth. Indeed (re)-absorption was higher using exciting lines at 647.1 and 785 nm than those at 457.9 and 514.5 nm. Therefore, resonance Raman spectroscopy probed a thinner layer even if it cannot be considered as surface characterization technique.

Fig. 3 compares the Raman spectra at 514.5 and 647.1 nm of $\mathrm{Cs_2Te_{0.2}V_{0.1}}$ sample before and after reaction. For this vanadium containing sample, the additional bands were observed both before and after reaction but with a much weaker relative intensity using the laser line at 514.5 nm. The observation of the additional bands before and after reaction can be related to the existence of d–d and IVCT transitions in both cases as shown in the previous part. Interestingly, the relative intensities of the main additional band near 540 $\mathrm{cm^{-1}}$ were rather close for the spectra achieved at 514.5 nm after reaction (Fig. 3b) and at 647.1 nm (Fig. 3c) before reaction. This band corresponds to diffused photons with wavelength at 529.2 and 670.5 nm using exciting lines at 514.5 and 647.1 nm, respectively. In parallel, the FR values corresponding to these wavelengths and determined from Fig. 1 were very close (2.42 and 2.41, respectively). Therefore, it seems that the relative intensity of the Raman band at 540 $\mathrm{cm^{-1}}$ is mainly determined by absorption and hence the penetration depth. In fact, this parameter strongly depends on the FR value and consequently, on the inverse of the penetration depth. Indeed, it was much weaker in the Raman spectrum at 514.5 nm of $\mathrm{Cs_2Te_{0.2}V_{0.1}}$ sample before reaction (Fig. 3a) than after reaction (Fig. 3b) whereas the FR values at 529.2 nm were 1.47 and 2.41, respectively. On the other hand, it was much higher in the Raman spectrum at 647.1 nm after reaction (Fig. 3d) than before reaction (Fig. 3c) when the FR value at 670.5 nm only increased from 2.42 to 3.21. This quick variation can be explained by the presence of an absorbing layer of reduced molybdenum species lying over unreduced $[\mathrm{PMo_{12}O_{40}}]^{3-}$ in the $\mathrm{Cs_2Te_{0.2}V_{0.1}}$ sample. Then, the response of the inner Keggin phase would strongly depend on the penetration depth compared to the thickness of the upper layer and dramatically decrease when the incident light cannot probe it.

3.3. Attribution of the additional bands

Mestl et al. mentioned the observation of Raman bands at 825, 731, 675, 618, 544, 500, 470, 418, 388, 357 $\mathrm{cm^{-1}}$ on blue areas heterogeneously present in $\mathrm{PVMo_{11}}$ sample treated in mixture of $\mathrm{He/H_2O}$ at 430 °C using exciting line at 633 nm [15]. These positions are rather close to those of some additional bands reported in bold in Table 1. Specific observation on blue areas confirms that additional bands are due to reduced molybdenum species.

The observation of numerous additional bands is a good indication that the symmetry of reduced species is low. Two distinct groups of bands can be distinguished in the spectra: the first one ranging from 500 to 900 cm^{-1} contains broad and intense bands that can be attributed to $\nu(Mo^{5+}–O–Mo^{6+})$ or $\nu(Mo^{5+}–O–Mo^{5+})$ stretching vibrations. In the second one, spreading from 200 to 500 cm^{-1}, much thinner bands were observed. These bands can be tentatively assigned to $\delta(Mo^{5+}–O–Mo^{6+})$ or $\delta(Mo^{5+}–O–Mo^{5+})$ vibrations. As mentioned above, some of them were slightly enhanced using exciting lines at 647.1 and 785 nm and consequently, they are more sensitive to the electronic structure.

The spectrum composed of the additional bands was compared with the Raman spectra of mixed valence molybdenum oxides and reduced phosphomolybdates from the literature data and preparing some reference samples. In particular, as EXAFS results indicated that $[TeO_4]$ clusters with rather short Te–O bonds lengths of 1.93 Å were capping [13], we tried to prepare crystalline salts containing strongly reduced heteropolyanions capped by tellurium in order to get the corresponding Raman spectra after checking of the crystalline structure but without success. In fact, the best fit was obtained with the $(MoO_2)_{0.5}PMo_{14}O_{42}$ reference sample that has been proposed by Marosi et al. to contain six-electron reduced $[PMo_{12}O_{40}]^{9-}$ anions capped by two $(Mo = O)^{4+}$ molybdyl groups [16,17]. Indeed, very similar ν(Mo–O–Mo) bands were observed between 500 and 900 cm^{-1} as shown in Fig. 4. As for the $Cs_2Te_{0.5}$ sample, numerous thin bands were observed in the $(MoO_2)_{0.5}PMo_{14}O_{42}$ compound between 270 and 500 cm^{-1} but however, with some discrepancies. In particular, an intense band was present at 495 cm^{-1} in the reference sample whereas it was absent in the spectrum of $Cs_2Te_{0.5}$ compound. These discrepancies could arise from different enhancements arising from different electronic states in the two samples. Additionally, two bands at 1037–1048 cm^{-1} due to stretching vibrations of very short (Mo=O) bonds were clearly evidenced in the $(MoO_2)_{0.5}PMo_{14}O_{42}$ compound whereas no peak was distinguished in this range for the $Cs_2Te_{0.5}$ catalyst suggesting the absence of such (Mo=O) bonds.

Intense and broad ν(Mo–O–Mo) stretching vibrations in the 500–900 cm^{-1} range and numerous thin bands between 270 and 500 cm^{-1} were also observed in the four electron reduced $TBA_7[PMo_{12}O_{40}]$ sample (Fig. 4c). Such features could be common to reduced polyoxometalates.

3.4. *Influence of the $Cs_2Te_xV_z$ composition on the resonance Raman spectra and relationships with catalytic properties*

The Raman spectra of various $Cs_2Te_xV_z$ catalysts before reaction were achieved using exciting line at 647.1 nm. They are gathered in Fig. 5. The Raman spectra of Cs_2H and Cs_2Te_x samples (Fig. 5a–d) contained bands around 990, 975, 960, 880, 610, 385, 260 and 240 cm^{-1} typical of cesium phosphomolybdate salts. No additional bands were detected as already mentioned for the $Cs_2Te_{0.5}$ sample. On the contrary, the Raman spectrum $Cs_2Te_{0.2}V_{0.1}$ sample (Fig. 5e) revealed bands at 288, 490, 544, 660, 726, 779, and 844 cm^{-1} in addition to those of $[PMo_{12}O_{40}]^{3-}$. These features has to be linked

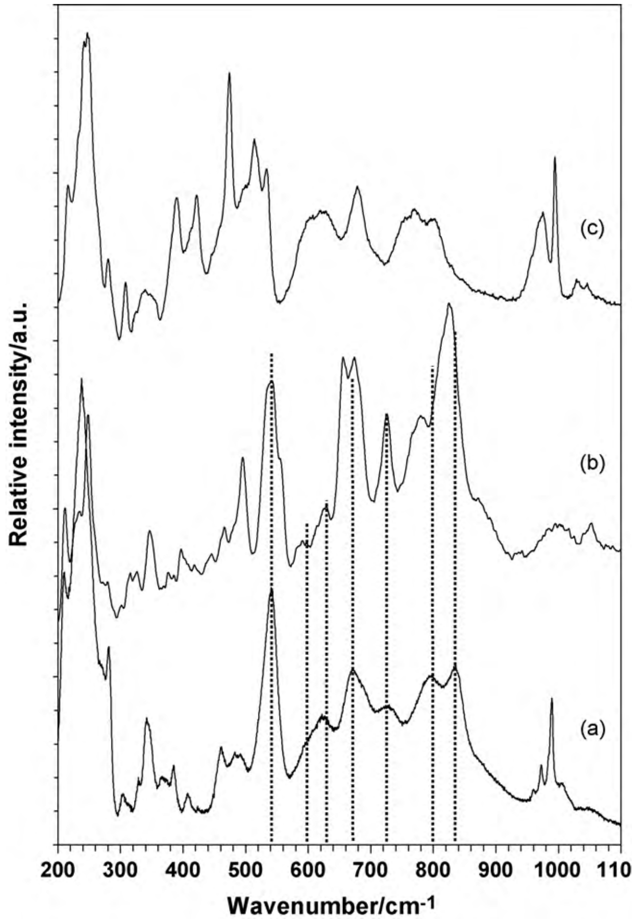

Fig. 4. Comparison of the Raman spectrum (647.1 nm) of: (a) $Cs_2Te_{0.2}V_{0.1}$ after reaction with those of (b) $(MoO)_{0.5}PMo_{14}O_{42}$ and (c) $TBA_7[PMo_{12}O_{40}]$ reference compounds.

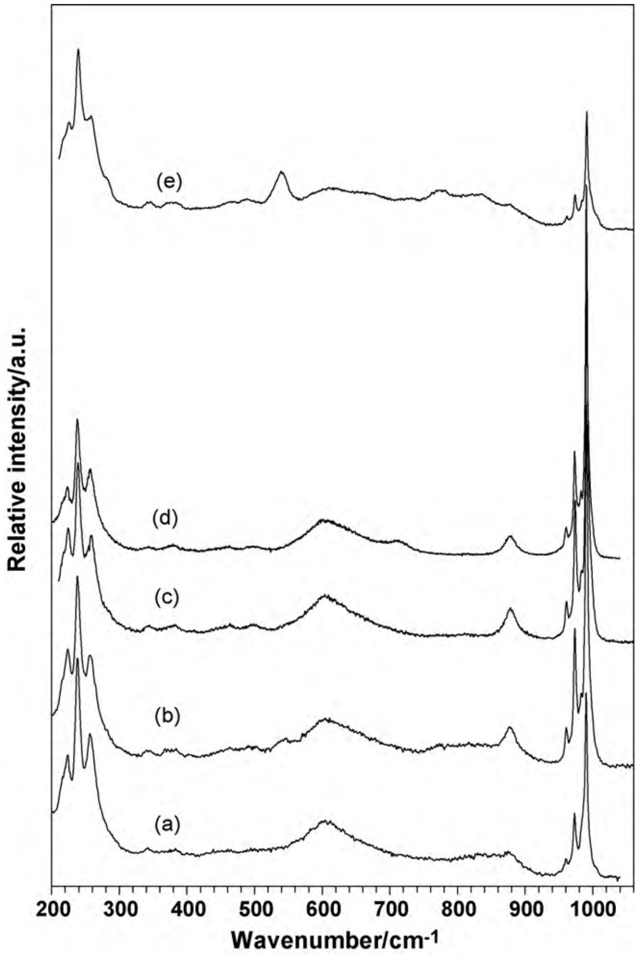

Fig. 5. Raman spectra (647.1 nm) before reaction of: (a) Cs_2H, (b) $Cs_2Te_{0.05}$, (c) $Cs_2Te_{0.2}$, (d) $Cs_2Te_{0.5}$ and (e) $Cs_2Te_{0.2}V_{0.1}$.

with the observation of d–d and IVCT bands in its diffuse reflectance spectrum (Fig. 1c) due to formation of Mo^{5+} cations after oxidation of V^{3+} to V^{4+} cations during the sample drying.

The Raman spectra of the various $Cs_2Te_xV_z$ catalysts after reaction are reported in Fig. 6: additional bands were evidenced in all the tellurium containing catalysts (Fig. 6b–e) and to a lesser extent in Cs_2H sample (Fig. 6a). The well-separated and intense band at 540 cm^{-1} was used for semi-quantitative analysis of reduced species. Its intensity was taken relative to that between 945 and 1030 cm^{-1} representative of $[PMo_{12}O_{40}]^{3-}$ anions. Fig. 7 plots the evolution of this relative intensity versus the tellurium content and clearly evidences a linear relation between the two parameters. This relationship reveals that the proportion of reduced species increases with the tellurium content and suggests that tellurium favours reduction. It cannot be a consequence of the catalytic activity since conversions slightly decreased with the tellurium amount in the Cs_2Te_x catalysts at a given testing temperature [13]. However, the presence of reduced species could improve the selectivity to MA and MAA that increased with the tellurium content at 350 °C and isoconversion (Fig. 7).

Unfortunately, it was not possible to evidence bands due to Te–O vibrations comparing the intensity of one additional band to the others for various compositions. Although the band at 282 cm^{-1} was absent in the Cs_2H sample (Fig. 6a) it cannot be attributed to vibrations involving tellurium cations since it was observed in the $TBA_7[PMo_{12}O_{40}]$ reference sample (Fig. 4c). In the same way, the band around 345 cm^{-1} was much weaker for the Cs_2H sample but cannot be attributed to tellurium cations since it was also observed in the $(MoO_2)_{0.5}PMo_{14}O_{42}$ reference sample (Fig. 4b). In fact, the low wavenumber bands could be mainly sensitive to the electronic properties of the reduced species and unfortunately, resonance Raman spectroscopy was not able to evidence a capping of reduced Keggin anions by $[TeO_4]$ clusters as suggested by EXAFS [13].

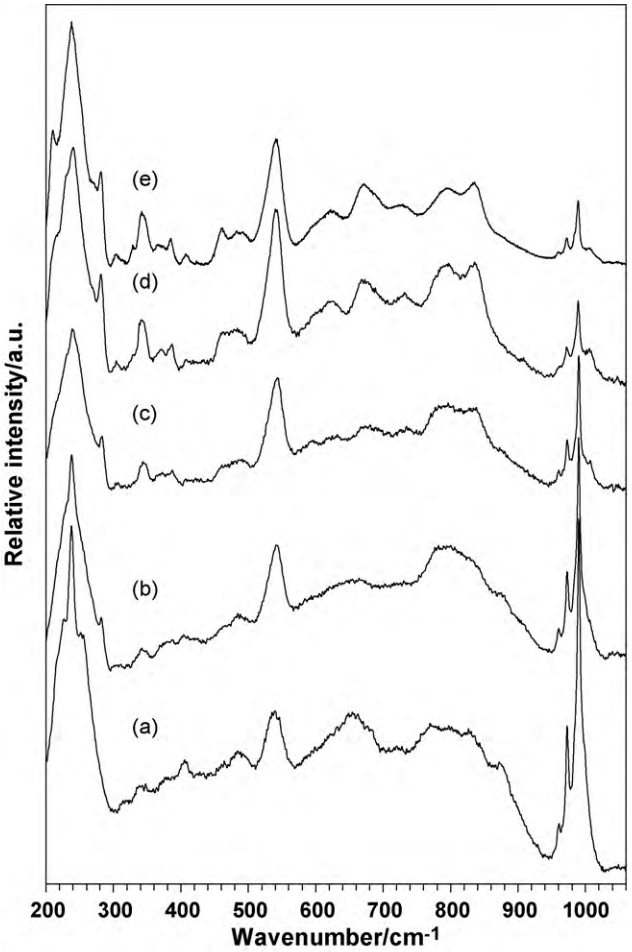

Fig. 6. Raman spectra (647.1 nm) after reaction of: (a) Cs_2H, (b) $Cs_2Te_{0.05}$, (c) $Cs_2Te_{0.2}$, (d) $Cs_2Te_{0.5}$ and (e) $Cs_2Te_{0.2}V_{0.1}$.

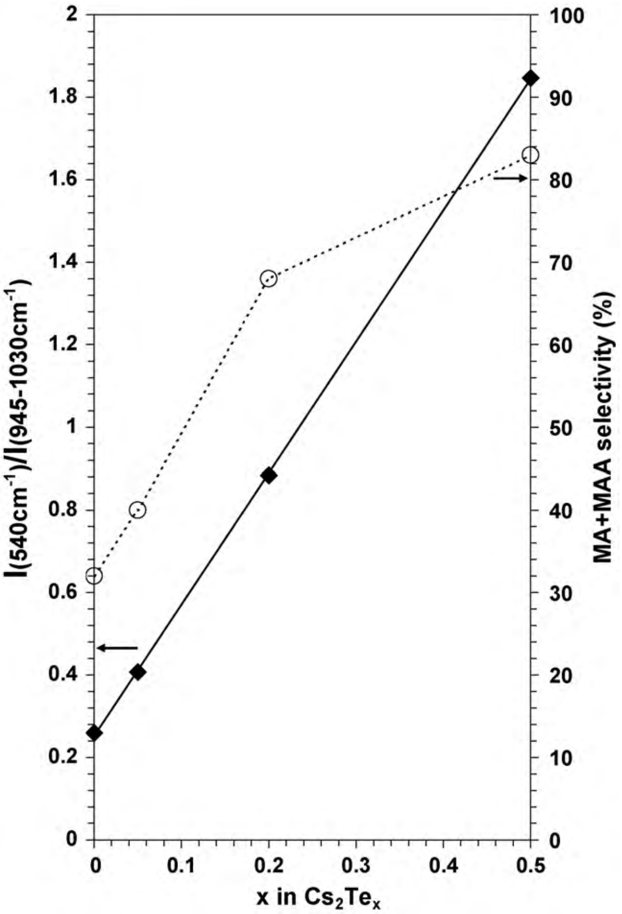

Fig. 7. Evolution with the tellurium content of: (◆) the intensity of the band at 540 cm^{-1} relative to that between 945 and 1030 cm^{-1} and (○) selectivity to MA + MAA at conversion 8–10% and at 350 °C.

3.5. *In situ and operando Raman experiments*

In situ Raman spectra were recorded on $Cs_2Te_{0.2}$ sample before reaction to evaluate the influence of temperature on the shape of spectra. Fig. 8 shows the evolution of spectra during thermal treatment up to 360 °C under air flow. When the temperature was raised, the Raman bands of $[PMo_{12}O_{40}]^{3-}$ anions were downshifted and broadened. The first phenomenon was due to weakening of force constants linked to the anharmonicity of the interatomic potential and the second one arises from the decay of one given phonon into two or three phonons [25]. The evolution of Raman spectra was perfectly reversible and in particular, no additional bands were observed after the thermal treatment.

Operando experiments were achieved on $Cs_2Te_{0.2}$ sample by coupling resonance Raman spectroscopy and GC–MS analysis. Fig. 9 shows the evolution of spectra when the temperature was raised under reaction mixture. The main catalytic data are summarized in Table 2. As during thermal treatment under air flow, the Raman bands of $[PMo_{12}O_{40}]^{3-}$ anions were downshifted and enlarged. Furthermore, it was shown that the additional bands observed after reaction (Fig. 6c) appeared around 120 °C under reaction mixture (Fig. 9b). This observation indicates that

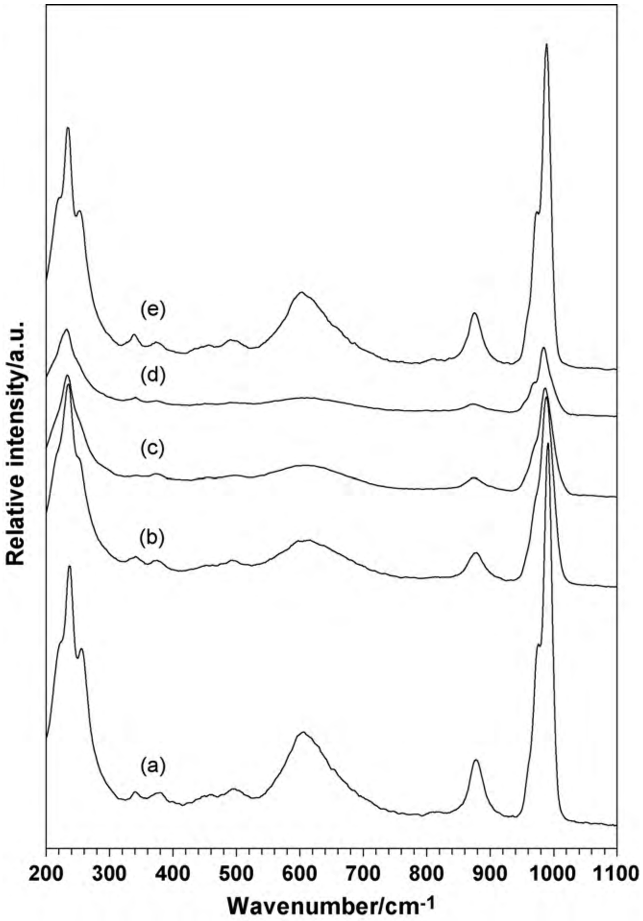

Fig. 8. In situ Raman spectra (647.1 nm) of $Cs_2Te_{0.2}$ sample achieved consecutively during thermal treatment under air flow at (a) 20 °C, (b) 200 °C, (c) 300 °C, (d) 360 °C and (e) 20 °C.

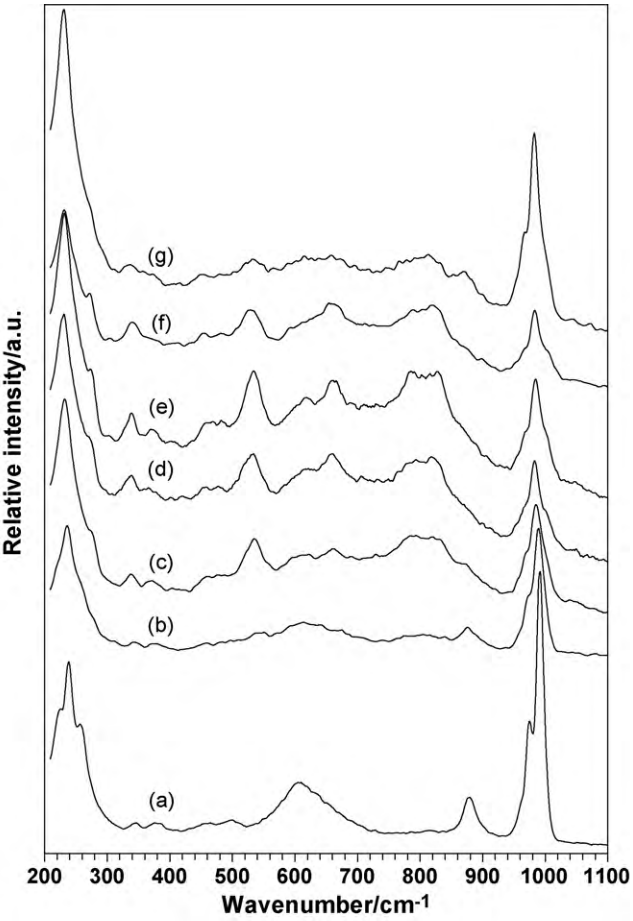

Fig. 9. Operando Raman spectra (647.1 nm) of $Cs_2Te_{0.2}$ sample (m = 757 mg) achieved consecutively under feed ($iC_4H_{10}/O_2/H_2O/He$ = 27/13.5/10/49.5, total flow rate = 20 ml min^{-1}) at: (a) 20 °C, (b) 138 °C, (c) 274 °C, (d) 336 °C, (e) 274 °C, (f) 376 °C and under O_2 flow at (g) 376 °C.

reduction of Keggin anions occurred from this temperature and was favoured by dehydration as previously reported for $H_{3+n}PV_nMo_{12-n}O_{40}$ compounds [26]. Increasing the temperature, the additional bands became progressively more intense compared to the bands of $[PMo_{12}O_{40}]^{3-}$ anions. At 336 °C, they were present (Fig. 9d) when small activity of the catalyst was measured (Table 2). The reactor temperature was then cooled down at 274 °C; temperature at which the catalyst was inactive. At this step, the additional bands were observed with a higher relative intensity (Fig. 9e) than during the first temperature raise (Fig. 9c). It suggests irreversible stabilization of reduced species increasing the temperature under reaction mixture. The temperature was then raised at 376 °C: the catalyst became undoubtedly active and selective to methacrolein and methacrylic acid (Table 2) and the additional bands were observed at the same time (Fig. 9f). By comparison with the spectrum achieved at 336 °C (Fig. 9d), no significant increase in their relative intensity was remarked.

After evidencing the presence of additional bands when the catalyst was working, the gas flow was switched to pure O_2: a quick and strong damping of the additional bands was then observed after few seconds (Fig. 9f). This evolution can be explained by increase in the penetration depth and decrease in the resonance effect. Such phenomenon was also observed for all the samples after reaction during thermal treatment under air flow: the additional bands observed at room temperature progressively vanished when the temperature was raised up to 360 °C and reappeared reversibly when the temperature was lowered. On the contrary, the additional bands were observed up to 360 °C under He flow for the samples after reaction. These evolutions emphasize the importance of the redox power of the gas phase on stabilization of reduced species.

Operando experiments were also achieved with $Cs_2Te_{0.2}V_{0.1}$ sample. Main Raman spectra are gathered in Fig. 10 and the main catalytic data are given in Table 2. As above-explained, additional bands at 490, 544, 652, 722, 777, 844 and 1055 cm^{-1} were already present at room temperature for this sample (Fig. 10a). No significant change was observed when the atmosphere was switched from ambient air to reaction mixture at room temperature. However, when the temperature was raised, the intensity of the additional bands was increased compared to that of $[PMo_{12}O_{40}]^{3-}$ anion confirming stabilization of reduced species under reaction mixture. As shown in Fig. 10c, these species were observed at 362 °C; temperature at which the catalyst was active and selective in the Raman cell (data in Table 2). Additionally, the relative intensity of the additional bands was kept constant decreasing the temperature at 289 °C confirming the irreversible stabilization of reduced species at moderate temperatures (Fig. 10d).

Finally, it is important to mention that no carboneous species were detected during the two operando experiments. The MA + MAA selectivities were lower than in conventional reactor probably because of the geometry of the operando reactor favouring deeper oxidation. The activities of $Cs_2Te_{0.2}$ and $Cs_2Te_{0.2}V_{0.1}$ catalysts are compared in Table 2. The conversion of the vanadium containing sample was slightly higher using lower mass and at lower temperature. It confirms that substitution by vanadium improves the catalytic activity [13].

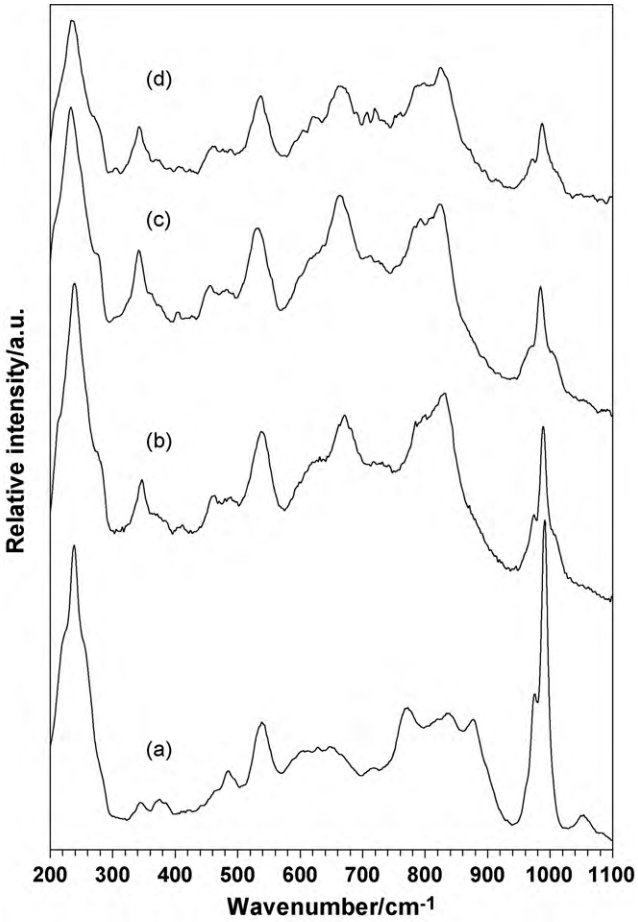

Fig. 10. Operando Raman spectra (647.1 nm) of $Cs_2Te_{0.2}V_{0.1}$ sample (m = 603 mg) achieved consecutively under feed ($iC_4H_{10}/O_2/H_2O/He = 27/13.5/10/49.5$, flow rate = 20 ml min^{-1}) at: (a) 20 °C, (b) 289 °C, (c) 362 °C and (d) 289 °C.

4. Discussion

It was shown, in our previous study, that the Raman spectra of the best $Cs_2Te_xV_y$ catalysts contained, after reaction, small bands in addition to those of $[PMo_{12}O_{40}]^{3-}$ using exciting line at 514.5 nm [13]. In the present investigation, we clearly observed these bands with much better sensitivity using exciting lines at 647.1 and 785 nm. This phenomenon cannot be explained only by resonance effect due to the existence of d–d and IVCT electronic transitions since, for instance, acquisition times remained rather long. In fact, strong (re)-absorption occurred in these reduced samples limiting the probed depth. As the average size of primary particles of samples was estimated around 120 nm by SEM and as additional bands were not observed by other bulk techniques (XRD, IR, NMR), one can consider that resonance Raman spectroscopy probes only few layers in the upper part of particles and hence is very suitable to characterize active sites.

The additional bands can be attributed to reduced heteropolymolybdates. The presence of capping TeO_4E entities with one lone pair (E) stereochemically active and four rather short Te–O bonds (1.93 Å) was previously proposed from EXAFS results [13]. Unfortunately, no direct proof of the capping was evidenced by resonance Raman spectroscopy in the present study. Possible explanations are that the tellurium amounts are too low and that mainly (Mo^{5+}–O–Mo^{6+}) or (Mo^{5+}–O–Mo^{5+}) vibrations were enhanced using laser exciting lines close to d–d transitions in Mo^{5+} cations and intervalence Mo^{5+}–Mo^{6+} charge transfers.

However, the relative intensity of the main additional band around 540 cm^{-1} increased linearly with the tellurium content in the samples after reaction. As the enhancement of additional bands depends on the number of Mo^{5+} cations, this evolution probably arises from higher degree of reduction of heteropolyanions favoured by the presence of Te^{4+} in a similar way than Sb^{3+} [12,27,28]. The presence of highly reduced anions was also confirmed by diffuse reflectance spectra that showed that Cs_2Te_x and $Cs_2Te_xV_z$ samples were more reduced than Cs_2H sample after reaction. By analogy with other capped phosphomolybdates, one can suggest that high degree of reduction is the driving force for the capping by Te^{4+} cations [29,30].

The formation of partially reduced lacunary Keggin anions in $Cs_2H[PMo_{12}O_{40}]$ by migration of molybdenum onto interstitial sites was proposed to occur in reducing atmospheres above 300 °C [31]. The driving force for the partial decomposition of Keggin anions would be thermal strain at elevated temperatures. Interestingly, the XRD pattern attributed to a cubic $Mo_zH_{3-x}[PMo_{12-z}O_{40-x/2}]$ phase was very close to that reported by Marosi et al. [17] and attributed to $(MoO_2)_{0.5}[PMo_{14}O_{42}]$ phase containing bi-capped Keggin anions. A major difference between the two attributions is that the number of Mo^{5+} cations was shown to be low in $Mo_zH_{3-x}[PMo_{12-z}O_{40-x/2}]$ phase whereas $[PMo_{14}O_{42}]^-$ Keggin anions are six-electron reduced.

Raman spectra of solutions containing lacunary $[PMo_{11}O_{39}]^{7-}$ and $[PMo_9O_{31}(OH)_3]^{3-}$ anions have been previously reported [32]. As for $[PMo_{12}O_{40}]^{3-}$, the main bands attributed to ν(Mo=O) stretching vibrations were observed between 950 and 1000 cm^{-1}. Between 600 and 800 cm^{-1}, $[PMo_9O_{31}(OH)_3]^{3-}$ revealed bands at 715 and 650 cm^{-1} whereas no band was observed for $[PMo_{11}O_{39}]^{7-}$. These spectra do not correspond to additional bands that were observed both in resonance and non-resonance conditions. Therefore, if $[PMo_{11}O_{39}]^{7-}$ and $[PMo_9O_{31}(OH)_3]^{3-}$ were present in the Cs_2Te_x and $Cs_2Te_xV_z$ compounds, it was in very limited amount. Additionally, if $[PMo_{11}O_{39}]^{7-}$ anions were present, they should be complexed by Te^{4+} cations. However, M^{4+}–O distances were reported to be higher than 2.15 Å in various Keggin and lacunary phosphomolybdates complexed by tetravalent metals [33,34]. Such distances are inconsistent with the average Te^{4+}–O distances determined by EXAFS to be only 1.93 Å in the tellurium substituted catalysts [13].

Another possibility is that the reduced species giving the additional bands would be lacunary. However, the existence of crystalline salts containing such anions has not been reported in the literature and in any case, they should contain several oxygen vacancies to own a reasonable negative charge.

From all these considerations, our attribution of the additional bands to highly reduced capped Keggin anions with formulas $[PMo^{5+}_{6+x}Mo^{6+}_{6-x}O_{40}M^{4+}_2]^{-1-x}$ or $[PMo^{5+}_{4+x}Mo^{6+}_{8-x}O_{40}M^{4+}]^{-3-x}$ (with

Table 2
Catalytic data determined during operando experiments of $Cs_2Te_{0.2}$ and $Cs_2Te_{0.2}V_{0.1}$ samples by coupling resonance Raman spectroscopy and GC/MS analysis. Composition of the reaction mixture: $iC_4H_{10}/O_2/H_2O/N_2 = 27/13.5/10/49.5$, flow rate = 20 ml min^{-1}. MA: methacrolein, MAA: methacrylic acid.

Compound	Mass (mg)	Temperature (°C)	iC_4H_{10} conversion (%)	O_2 conversion (%)	S (MA + MAA) (%)
$Cs_2Te_{0.2}$	757	336	2–3	10	–
		376	5.5	22	42
$Cs_2Te_{0.2}V_{0.1}$	602	362	6	32	49

M = Te^{4+} or $(VO)^{2+}$) was kept as previously reported [13] but has to be confirmed.

It has been shown that reduction of the average Mo valence coincides with the onset of catalytic activity for $H_4[PVMo_{11}O_{40}]$ precursors [35]. In the present study, reduction of Mo^{6+} cations was observed at much lower temperatures than the onset of catalytic activity since the reduced species started to be stabilized under reaction mixture from 120 °C for Cs_2Te_x catalysts and from room temperature for $Cs_2Te_xV_y$ catalysts. Such low reduction temperatures confirm that substitution of protons by Te^{4+} cations favours reduction of polyoxometalate (POM) under reaction mixture improving the selectivity to MA and MMA in similar way than substitution by Sb^{3+} [27,28,36]. It also confirms the importance of having reduced POM to reach high selectivities to oxygenated products from light alkanes [36–39]. Additionally, bands corresponding to the reduced species were observed by resonance Raman spectroscopy when the catalysts were active and selective. It does not prove that they are active species since they could be only spectator. However, a strong interaction between tellurium and vanadium cations and reduced anions is probably favoured by the high negative charge of the last ones that could lead to the existence of functionalized clusters able to activate isobutane, achieve oxidative dehydrogenation and oxygen insertion steps. Additionally, in the present study, a relationship was established between the relative intensity of the bands arising from reduced species and the selectivity to MA and MAA. These features strongly suggest that reduced species containing tellurium cations are active and more selective sites.

5. Conclusion

Resonance Raman spectroscopy is very powerful to specifically insight reduced species present in Cs_2Te_x and $Cs_2Te_xV_y$ catalysts thanks to a much better sensitivity. Indeed, in the present investigation, an impressive enhancement of additional bands due to these species was evidenced using exciting lines at 647.1 and 785 nm when the wavelength of the laser was close to those d–d and IVCT transitions. This phenomenon was explained mainly by decrease in the probed depth allowing characterization of the upper part of particles and to a lesser extent, by resonance effect. The additional bands were attributed to highly reduced heteropolymolybdates. Reduction was shown to be favoured by the presence of tellurium that leads also to increase in the selectivities to MA and MAA. Unfortunately, no proof of the capping by Te^{4+} or $(V{=}O)^{2+}$ cations was obtained by resonance Raman spectroscopy using exciting line at 647.1 nm. It could arise from specific enhancement of $(Mo^{5+}–O–Mo^{6+})$ and $(Mo^{5+}–O–Mo^{5+})$ vibrations in resonance conditions. For Cs_2Te_x catalysts, reduced species were formed around 120 °C during activation under reaction mixture. For $Cs_2Te_xV_y$ catalysts, small amount of these species was already observed after drying but the main part was also formed during the thermal activation.

The additional bands were observed by operando resonance Raman spectroscopy when the catalysts were active and selective to MA and MAA. This feature and the relationship established between the relative intensity of the additional bands and the selectivity to MA and MAA strongly suggest that reduced phosphomolybdates stabilized under gas mixture at the reaction temperature are active and more selective sites.

Acknowledgements

S. Prakash is acknowledged for his help during UV–vis experiments. The authors thank also Pr.G. Lucazeau and Pr.E. Cadot for fruitful discussions on resonance Raman scattering and capped reduced heteropolyanions, respectively.

References

[1] M.A. Banares, Catal. Today 100 (1–2) (2005) 71–77.
[2] B.M. Weckhuysen, Phys. Chem. Chem. Phys. 5 (20) (2003) 4351–4360.
[3] M.A. Banares, G. Mestl, Adv. Catal. 52 (2009) 43–128.
[4] M. Dieterle, G. Weinsberg, G. Mestl, Phys. Chem. Chem. Phys. 4 (2002) 812–821.
[5] M. Dieterle, G. Mestl, Phys. Chem. Chem. Phys. 4 (2002) 822–826.
[6] G. Ricchiardi, A. Damin, S. Bordiga, C. Lamberti, G. Spano, R. Guido, F. Rivetti, A. Zecchina, J. Am. Chem. Soc. 123 (46) (2001) 11409–11419.
[7] H.-S. Kim, P.C. Stair, J. Phys. Chem. A 113 (16) (2009) 4346–4355.
[8] A. Damin, F. Bonino, S. Bordiga, E. Groppo, C. Lamberti, A. Zecchina, Chem. Phys. Chem. 7 (2) (2006) 342–344.
[9] C. Li, J. Catal. 216 (1–2) (2003) 203–212.
[10] O. Demoulin, M. Navez, E.M. Gaigneaux, P. Ruiz, A.-S. Mamede, P. Granger, E. Payen, Phys. Chem. Chem. Phys. 5 (2003) 4394–4401.
[11] Q. Huynh, P. Lacorre, J.M.M. Millet, French Patent 0,601,284 (2006).
[12] F. Cavani, R. Mezzogori, A. Pigamo, F. Trifiro, Top. Catal. 23 (1–4) (2003) 119–124.
[13] Q. Huynh, Y. Schuurman, P. Delichere, S. Loridant, J.M.M. Millet, J. Catal. 261 (2009) 166–176.
[14] M. Langpape, J.M.M. Millet, U.S. Ozhan, M. Boudeulle, J. Catal. 181 (1999) 80–90.
[15] G. Mestl, T. Ilkenhans, D. Spielbauer, M. Dieterle, O. Timpe, J. Kröhnert, F. Jentoft, H. Knözinger, R. Schlögl, Appl. Catal. A: Gen. 210 (2001) 13–24.
[16] L. Marosi, J. Cifre, C.O. Arean, Powder Diffraction 18 (3) (2003) 236–239.
[17] L. Marosi, C.O. Arean, J. Catal. 213 (2003) 235–240.
[18] J.N. Barrows, T. Michael, Adv. Chem. Ser. 226 (1990) 403–417.
[19] H. Launay, S. Loridant, D.-L. Nguyen, A.M. Volodin, J.-L. Dubois, J.M.M. Millet, Catal. Today 128 (2007) 176–182.
[20] R.I. Buckley, R.J.H. Clark, Coord. Chem. Rev. 65 (1985) 167–218.
[21] S. Klokishner, J. Melsheimer, R. Ahmad, F.C. Jentoft, G. Mestl, R. Schögl, Spectrochim. Acta Part A 58 (2002) 1–15.
[22] C. Sanchez, J. Livage, J.P. Launay, M. Fournier, Y. Jeannin, J. Am. Chem. Soc. 104 (1982) 3194–3202.
[23] J. Melsheimer, J. Kröhnert, R. Ahmad, S. Klokishner, F.C. Jentoft, G. Mestl, R. Schlögl, Phys. Chem. Chem. Phys. 4 (2002) 2398–2408.
[24] A.J. Bridgeman, Chem. Phys. 287 (2003) 55–69.
[25] G. Lucazeau, J. Raman Spectrosc. 34 (7/8) (2003) 478.
[26] J.K. Lee, J. Melsheimer, S. Berndt, G. Mestl, R. Schlögl, K. Köhler, Appl. Catal. A: Gen. 214 (2001) 125–148.
[27] F. Cavani, R. Mezzogori, A. Pigamo, F. Trifiro, Stud. Surf. Sci. Catal. 140 (2001) 141–152.
[28] F. Cavani, A. Tanguy, F. Trifiro, M. Koutrev, J. Catal. 174 (1998) 231–241.
[29] C. Qin Chen, C.L. Hill, Inorg. Chem. 35 (1996) 2403.
[30] S. Chang, C. Qin, X.-L. Wang, Y.-G. Li, E.-B. Wang, Chem. Res. Chin. Univ. 22 (1) (2006) 17–20.
[31] J. Wienold, O. Timpe, T. Ressler, Chem. Eur. J. 9 (2003) 6007–6017.
[32] J.A. Rob van Veen, O. Sudmeijer, C.A. Emeis, H. de Wit, J. Chem. Soc. Dalton Trans. (1986) 1825–1831.
[33] R. Copping, L. Jonasson, A.J. Gaunt, D. Drennan, D. Collison, M. Helliwell, R.J. Pirttijarvi, C.J. Jones, A. Huguet, D.C. Apperley, N. Kaltsoyannis, L. May, Inorg. Chem. 47 (2008) 5787–5798.
[34] A.J. Gaunt, I. May, D. Collison, O.D. Fox, Inorg. Chem. 42 (2003) 5049–5051.
[35] T. Ressler, O. Timpe, F. Girgsdies, J. Wienold, T. Neisius, J. Catal. 231 (2005) 279–291.
[36] F. Cavani, R. Mezzogori, A. Pigamo, F. Trifiro, E. Etienne, Catal. Today 71 (2001) 97–110.
[37] F. Cavani, R. Mezzogori, A. Pigamo, F. Trifiro, Chem. Eng. J. 82 (2001) 33–42.
[38] W. Ueda, Y. Suzuki, Chem. Lett. 7 (1995) 541–542.
[39] W. Li, K. Oshihara, W. Ueda, Appl. Catal. A: Gen. 182 (1999) 357–363.